Conformal Invariance and Stochastic Loewner Evolution Processes in Two-Dimensional Ising Spin Glasses

C. Amoruso,[1] A. K. Hartmann,[2] M. B. Hastings,[3] and M. A. Moore[1]

[1]*School of Physics and Astronomy, University of Manchester, Manchester M13 9PL, United Kingdom*

[2]*Institut für Theoretische Physik, Universität Göttingen, Friedrich-Hund-Platz 1, 37077, Göttingen, Germany*

[3]*Center for Nonlinear Studies and Theoretical Division, Los Alamos National Laboratory, Los Alamos, New Mexico 87545, USA*

(Received 31 January 2006; revised manuscript received 12 July 2006; published 26 December 2006)

We present numerical evidence that the techniques of conformal field theory might be applicable to two-dimensional Ising spin glasses with Gaussian bond distributions. It is shown that certain domain wall distributions in one geometry can be related to that in a second geometry by a conformal transformation. We also present direct evidence that the domain walls are stochastic Loewner (SLE) processes with $\kappa \approx 2.1$. An argument is given that their fractal dimension d_f is related to their interface energy exponent θ by $d_f - 1 = 3/[4(3 + \theta)]$, which is consistent with the commonly quoted values $d_f \approx 1.27$ and $\theta \approx -0.28$.

DOI: 10.1103/PhysRevLett.97.267202 PACS numbers: 75.10.Nr, 05.50.+q, 11.25.Hf, 75.50.Lk

The powerful tools provided by conformal field theory (CFT) have permitted the determination of the exponents associated with most two-dimensional (2D) critical phenomena [1]. Unfortunately, CFT has not to date provided any results on systems like spin glasses, which in two dimensions have a zero temperature transition, i.e., $T_c = 0$. As the temperature of the system T is reduced to zero, the correlation length ξ increases to infinity [2,3] as $\xi(T) \sim 1/T^{\nu}$. The Hamiltonian of the system is $H = -\sum_{\langle ij\rangle} J_{ij} S_i S_j$, with $S_i = \pm 1$. If the nearest-neighbor bond distribution J_{ij} is continuous, as in the Gaussian distribution, then the exponent $\nu = -1/\theta$, where θ is the exponent which describes how the energy ΔE of a domain wall (DW) which crosses a system of linear extent L depends upon L: $\Delta E \sim L^{\theta}$ [3]. According to numerical studies [4,5] θ lies between -0.28 and -0.29. The DW has a fractal dimension $d_f \approx 1.27 \pm 0.01$ [6]. While the disorder present in spin glasses means that at a local level there is not even translational invariance, the existence of a diverging length scale such as $\xi(T)$ suggests that on long length scales such microscopic features could become irrelevant and that possibly even conformal invariance (CI) might arise. It is the chief purpose here to provide numerical evidence that this is indeed the case and so hopefully pave the way to eventually determining exponents like θ using CFT.

In the first part of this Letter we present a numerical study of whether there is conformal invariance of the DW distribution in 2D spin glasses. Within our numerical accuracy, CI does seem to hold in the thermodynamic limit. Then we next present numerical evidence that DWs in 2D are stochastic Loewner evolution (SLE) processes [7], and finally we suggest a relationship between θ and d_f.

CI of the DW distribution implies that given two geometries related by a conformal transformation, then the probability of finding the DW in a given configuration in one geometry is related to the probability of finding the conformally transformed DW configuration in the transformed geometry. We will find a transformation $F(z)$ mapping the geometry of Fig. 1(a) onto Fig. 1(d). The two rectangles have periodic boundary conditions so that the left and right edges are identified, while the top and bottom edges are open; i.e., they have the topology of an annulus. The two slits in Fig. 1(d) also have open boundary conditions, so that no bonds cross the slits. The rectangle 1(a) has an arbitrary aspect ratio; we can tune the distance between the slits in Fig. 1(d) as desired, with the aspect ratio of the right rectangle being a function of the distance between the slits and the aspect ratio of the left rectangle as given implicitly by Eq. (3). The dashed and dotted lines in each geometry are also conformally mapped to each other.

Before presenting the desired conformal mapping, we discuss the implications of CI in these geometries. First, we present the implications of conformal invariance for the probability distribution of the domain wall in these two geometries. We can measure the probability $p_1(n)$ of the domain wall crossing the dashed line n times in the rectangle geometry, 1(a), as well as the probability $p_1'(n)$ of the domain wall crossing the line n times in the slit geometry, 1(d). In Fig. 1, we also show the mapping of a DW which crosses the dashed line 3 times. In addition, we can measure the probability $p_2(n)$ of the domain wall crossing the

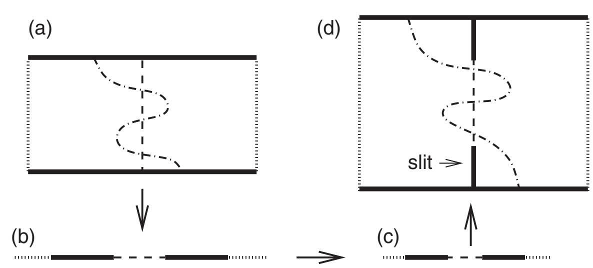

FIG. 1. Mapping between different geometries, and of the DW, shown as the dashed-dotted line.

dotted line n times in the rectangle geometry, as well as the probability $p_2'(n)$ of n crossings in the slit geometry. By statistical translational invariance, this probability is equal to $p_1(n)$. Thus, a naive application of CI would suggest that $p_2'(n) = p_1'(n)$. However, in the continuum limit it is not possible to distinguish between n and $n+2$ crossings of the dashed line for $n \neq 0$; if the distance between successive crossings of the dashed line in Fig. 1 is of the order of the lattice spacing, this looks at large scale like a single crossing of the dashed line. Thus, the predictions of CI are

$$p_1' \equiv \sum_{n\text{even}} p_1'(n) = \sum_{n\text{even}} p_2'(n) \equiv p_2', \\ \sum_{n\text{odd}} p_1'(n) = \sum_{n\text{odd}} p_2'(n), \qquad p_1'(0) = p_2'(0). \tag{1}$$

These identities in Eq. (1) are the consequence of a conformal automorphism of the slit geometry which interchanges the dotted and dashed lines: $z \to F[F^{-1}(z) + \pi]$. We explicitly checked for a small rectangular system ($N = 30 \times 30$) that $p_1 = p_2 \sim 0.603$ and they are equal to p_2' (quoted in Tables I and II) within the statistical error.

Our main test for CI is to find whether $p_1' = p_2'$. The naive expectation is that the DW is less likely to cross the dashed line, due to the constriction reducing the number of possible configurations, while CI instead requires these probabilities to be equal.

Constructing the Conformal Transformation.—We define the rectangle 1(a) to have width 2π and height h, and thus aspect ratio $h/2\pi$. The horizontal direction as plotted is the real coordinate running from $-\pi$ to π while the vertical is the imaginary coordinate, which runs from $-ih/2$ to $ih/2$. We define $\tau(h) = 2\pi i/h$, and $\lambda(\tau)$ to be the modular lambda elliptic function. We define a function $g(z)$ to map from Fig. 1(a) to Fig. 1(b) by

$$g_h(z) = \mathrm{sn}(2izK(\lambda(\tau(h)))/h|\lambda(\tau(h))), \tag{2}$$

where K is the complete elliptic integral of the first kind and sn is the Jacobi elliptic function [8]. This function g maps the dashed and dotted lines as shown. The dotted lines extend off to infinity and all lines lie on the real axis. The upper and lower lines of the rectangle are mapped to the two solid lines, which have endpoints at ± 1 and $\pm 1/\sqrt{\lambda(\tau(h))}$.

The mapping from 1(b) to 1(c) is simply $z \to sz$, for some parameter $0 < s \leq 1$; smaller values of s produces deeper cuts into the rectangle in 1(d). In 1(c), the endpoints of the lines are at $\pm s$ and $\pm s/\sqrt{\lambda(\tau)}$. We then determine the height h' of the rectangle in (d) such that

$$1/\sqrt{\lambda(\tau(h'))} = s/\sqrt{\lambda(\tau(h))}. \tag{3}$$

The final mapping from 1(c) to 1(d) is $z \to g_{h'}^{-1}(z)$. This maps the portion of the solid lines in 1(c) between ± 1 and $\pm 1/\sqrt{\lambda(\tau(h'))}$ onto the upper and lower borders of the rectangle in 1(d), while the portion of the solid lines in the third geometry between $\pm s$ and ± 1 are mapped onto the slits. Thus, the full mapping from 1(a) to 1(d) is

$$F(z) = g_{h'}^{-1}(sg_h(z)), \tag{4}$$

and the endpoints of the slits in 1(d) are located at $F(\pm ih/2)$.

We proceed by first finding the ground state of the system, using a mapping to a graph-theoretical problem, the minimum-weight perfect matching problem [9]. Domain walls were created by flipping the signs of the horizontal bonds in a column. Because of the periodicity in the horizontal direction, this induces a DW across the system and it is the crossings of the dashed central line and the dotted "end" line which we study. A DW is best defined as a walk on the lattice dual to the original lattice, and the dotted and dashed lines are also lines of this dual lattice.

In Tables I and II are displayed the values of p_1' and p_2' and the probabilities of zero crossings, $p_1'(0)$ and $p_2'(0)$ for $s = 0.95$ and $s = 0.90$ for various "sizes". Thus 30×32 means that the system studied is rectangular with 30 spins on each horizontal line (the direction in which the system is periodic) and 32 spins on each vertical line. The next number 8 is the number of rows cut by slits (4 at the top of the system, 4 at the bottom of the system) indicating that there are $(32 - 8)$ rows not cut by slits. (For small sizes it is not possible to find integers to get the sizes precisely correct for the given the aspect ratio).

For each probability p in these tables $\sqrt{[p(1-p)/N_s]}$ is its standard deviation, where N_s is the number of samples, i.e., bond realizations averaged over. As the size increases so the continuum limit is approached, the closer p_1' and p_2' become, implying that the distribution of the DWs is conformal. In Fig. 2 we have plotted p_1' versus $(1/L_1^{d_f-1})$ and p_2' versus $(1/L_2^{d_f-1})$. (We have no proof that this is the way that p_1' and p_2' approach their asymptotic limit, but this dependence will be partly motivated below). Again one can see that in the continuum limit CI seems to hold. L_1 is the number of rows not cut by the slit and L_2 is the total

TABLE I. Approach to CI for $s = 0.95$.

Size	p_1'	p_2'	$p_1'(0)$	$p_2'(0)$	samples
30 × 32; 8	0.624	0.603	0.463	0.409	20 000
52 × 55; 14	0.618	0.609	0.424	0.392	10 000
76 × 80; 20	0.616	0.615	0.417	0.385	10 000
98 × 103; 26	0.617	0.615	0.414	0.385	7000

TABLE II. Approach to CI for $s = 0.90$.

Size	p_1'	p_2'	$p_1'(0)$	$p_2'(0)$	samples
30 × 33; 12	0.639	0.604	0.494	0.407	20 000
50 × 56; 20	0.623	0.612	0.448	0.399	10 000
98 × 109; 38	0.620	0.611	0.421	0.384	6000
124 × 138; 48	0.612	0.610	0.411	0.381	6000

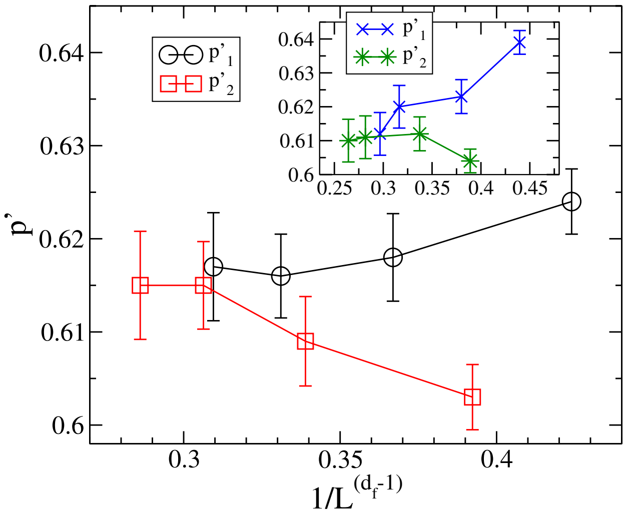

FIG. 2 (color online). Approach of p_1' and p_2' to asymptopia. Main figure is for $s = 0.95$ while inset for $s = 0.90$.

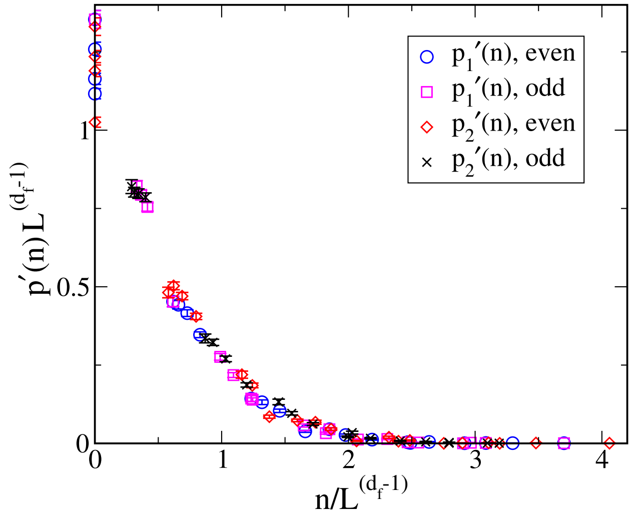

FIG. 3 (color online). Scaling of probability of crossings for $s = 0.95$.

number of rows in the system. Thus for the 30×32 system size, $L_1 = 24$ and $L_2 = 32$.

Unfortunately the probabilities for zero crossings $p_1'(0)$ and $p_2'(0)$ appear to approach each other very slowly (if at all). In an attempt to understand this behavior, we have studied the probabilities of n crossings, $p_1'(n)$, of the central (dashed) line, and $p_2'(n)$ of the right (dotted) line. $p_1'(n)$ has a scaling dependence on the number of crossings n as $(1/L_1^{d_f-1})f_a(n/L_1^{d_f-1})$ and similarly $p_2'(n)$ is of the form $(1/L_2^{d_f-1})f_a(n/L_2^{d_f-1})$. The subscript a is added (so $a = e$ or $a = o$) to allow us to distinguish even values of n from odd values, as the DW is topologically very different depending on the parity of n. $p_1'(n \neq 0)$ can mean that macroscopically the DW crosses the central line once (say), but then if one zooms in on that single crossing, it actually crosses many times. To see how many times it would cross, suppose the DW has fractal dimension d_f. Then, the intersection of the DW and a vertical line has dimension $d_f - 1$. Thus, the expected number of crossings would be $L_1^{d_f-1}$ which gives the above scaling forms. In Fig. 3 we display the data. The scaling functions for even and odd seem to be very similar, even though the DWs are topologically very different. Notice that the no-crossing probabilities are clearly not part of this scaling form (which they cannot be if they are nonzero). However, we suspect in the light of the above that the convergence of $p_1'(0)$ and $p_2'(0)$ to each other might be as slow as $(1/L^{d_f-1})$, and as d_f is about 1.27 this could be a very slow convergence rate. We have also studied the case of $s = 0.85$, which corresponds to a still deeper cut by the slits. For this case, the convergence of even p_1' to p_2' has not been achieved in the largest sizes we have studied (146×175), and we suspect that the slow convergence here is of similar origin.

The conformal invariance found in the DW distribution encouraged us to find out if the domain walls were also SLE processes [7]. Suppose the domain wall is the curve $\gamma(t)$ which begins at a point on the boundary of the upper half-plane H. The half-plane H minus the curve $\gamma(t)$ can be mapped back onto H by an analytic function $g_t(z)$ which is made unique by demanding that $g_t(z) \sim z + 2t/z + O(1/z^2)$ at infinity. The growing tip of the curve is mapped onto the real point $\xi(t)$. The DW is an SLE process if $\xi(t)$ is a Brownian walk whose elements have an independent Gaussian distribution and $\langle \xi(t)^2 \rangle = \kappa t$. The diffusion coefficient κ is of prime importance as it is related to the central charge of the conformal field theory [7]. In practice we approximate $g_t(z)$ by composing a sequence of discrete, conformal slit maps of the form $z \to \sqrt{(z - \xi_i)^2 + 4\Delta t_i} + \xi_i$, where the parameters Δt_i, ζ_i are chosen so that the ith such map removes the ith step from the domain wall following the procedures of Ref. [10], to produce a series of times $t_i = t_{i-1} + \Delta t_i$ and values $\xi(t_i) = \xi_i$ which ap-

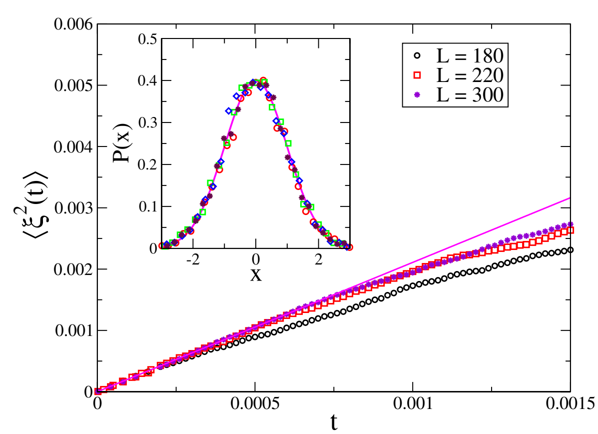

FIG. 4 (color online). $\langle \xi(t)^2 \rangle$ versus Loewner time t for three different system sizes L. The straight line has slope 2.1, which is our estimate for κ. Inset: probability distribution at four different times, 0.0003, 0.0004, 0.0005 and 0.0006 when $L = 300$. The curve is the Gaussian $\exp(-x^2)/\sqrt{2\pi}$, where $x = \xi(t)/\sqrt{\kappa t}$.

proximate $\xi(t)$. We denote the coordinates of the domain wall points by z_i^0, $i = 1\dots N$. The first such slit map transforms the coordinate of the first step, z_1^0, into the origin, and transforms z_j^0, $j > 1$, into a new point z_j^1. In general, the ith map transforms z_i^{i-1} into the origin and gives

$$t_i = t_{i-1} + (y_i^{i-1})^2/4, \qquad \xi(t_i) = x_i^{i-1},$$
$$z_j^i = \sqrt{[z_j^{i-1} - x_i^{i-1}]^2 + (y_i^{i-1})^2} + x_i^{i-1}, \qquad (j > i). \tag{5}$$

As usual the complex number $z = (x, y)$ and $\xi(t_0) = 0$. The sign of the square root is chosen so that it has the sign of $[x_j^{i-1} - x_i^{i-1}]$. The geometry which we studied was a square $L \times L$ with periodic boundary conditions in the horizontal direction and open boundaries in the vertical direction, which is the direction in which the domain runs. In Fig. 4 we show the average over realizations of the disorder of $\langle \xi(t)^2 \rangle$, plotted against t, for three values of L. When $L = 180$, we took 3000 disorder realizations; for $L = 220$, 4000; and for $L = 300$, 5000. $\langle \xi(t)^2 \rangle$ is linear in time for a range of times which increase with the system size L and from the slope of this linear region we estimate that $\kappa \approx 2.1$. Our boundary conditions, together with the finite size of the system, means that it does not properly satisfy the requirements for producing either chordal or dipolar SLE [7], which may partly explain the modest size of the linear regime. In a recent related study it was found that using the dipolar SLE did indeed extend the linear regime [11]. In the inset to Fig. 4 we show that the probability distributions of $\xi(t)/\sqrt{\kappa t}$ at four different times within the linear regime are standard Gaussian as would be required for the domain walls to be SLE processes.

If spin-glass domain walls are SLE processes, there may be a relationship between the fractal dimension of the DW d_f and the exponent θ. The fractal dimension is related to κ via $d_f = 1 + \kappa/8$ [7]. (Our numerical value for $\kappa \approx 2.1$ and the estimates of $d_f \approx 1.27 \pm 0.01$ in Ref. [6] are consistent with this relationship). The correlation length exponent ν is related to one of the Kac elements of conformal field theory: for example, in Potts models with components Q, $1 \leq Q \leq 4$, one has $d - 1/\nu = 2 + \theta = 2h_{2,1}$, but in other models $d - 1/\nu$ is $2h_{1,3}$ or $2h_{1,2}$. d is the dimensionality of the system, i.e., 2. Now if SLE applies, each of these elements is related to κ: $2h_{2,1} = (6 - \kappa)/\kappa$ [7], $2h_{1,3} = \kappa - 2$ etc. For each of these possibilities one can derive a relationship between d_f and θ and the only one which comes close to the numerical values $d_f = 1.27 \pm 0.01$ and $\theta = -0.285 \pm 0.05$ is from $2h_{2,1} = \frac{6-\kappa}{\kappa} = d - \frac{1}{\nu} = d + \theta$. Then on eliminating κ in favor of d_f gives

$$d_f = 1 + \frac{3}{4(3 + \theta)}. \tag{6}$$

On using one of the alternative possible relations, say $2 + \theta = 2h_{1,3}$, $d_f = (12 + \theta)/8$. Then the predicted value of $d_f = 1.46$ which is not consistent with its numerical value. Equation (6) seems to be the only possible relationship between d_f and θ which is compatible with their numerically well-established values. [Note that Eq. (6) would not apply to the $\pm$J spin-glass model as for it ν might have the same value as for the spin-glass model whose bonds have a Gaussian distribution [12] but it has $\theta = 0$ [13]]. The apparent success of Eq. (6) in providing a relationship between d_f and θ might provide a clue in finding the kind of conformal field theory appropriate for two-dimensional spin glasses. Our numerical evidence for conformal invariance and SLE strongly suggests that such a field theory should indeed exist.

We thank Antonio Celani, Andreas Honecker, Ron Fisch, and Marco Picco for fruitful discussions. We thank the authors of Ref. [11] for communicating the details of their numerous SLE investigations. This work was supported from the European Community via the DYGLAGEMEM contract. A. K. H. acknowledges financial support from the *VolkswagenStiftung* (Germany) within the program "Nachwuchsgruppen an Universitäten." M. B. H. was supported by DOE No. W-7405-ENG-36.

[1] P. Di Francesco, P. Mathieu, and D. Senechal, *Conformal Field Theory* (Springer, New York, 1997).
[2] H. G. Katzgraber, L. W. Lee, and A. P. Young, Phys. Rev. B **70**, 014417 (2004).
[3] A. J. Bray and M. A. Moore, in *Glassy Dynamics and Optimization*, edited by J. L. van Hemmen and I. Morgenstern (Springer, Berlin, 1986); D. S. Fisher and D. A. Huse, Phys. Rev. Lett. **56**, 1601 (1986); Phys. Rev. B **38**, 386 (1988); W. L. McMillan, J. Phys. C **17**, 3179 (1984).
[4] A. C. Carter, A. J. Bray, and M. A. Moore, Phys. Rev. Lett. **88**, 077201 (2002).
[5] A. K. Hartmann, A. J. Bray, A. C. Carter, M. A. Moore, and A. P. Young, Phys. Rev. B **66**, 224401 (2002).
[6] A. K. Hartmann and A. P. Young, Phys. Rev. B **66**, 094419 (2002).
[7] For a review aimed at physicists, see J. Cardy, Ann. Phys. (N.Y.) **318**, 81 (2005); M. Bauer and D. Bernard, Phys. Rep. **432** 115 (2006).
[8] Function $g_h(z)$ is related by a logarithmic map to one given in H. Kober, *Dictionary of Conformal Representations* (Dover, New York,1957), section 13.11, p. 192.
[9] A. K. Hartmann and H. Rieger, *Optimization Algorithms in Physics* (Wiley-VCH, Berlin, 2001).
[10] D. Bernard, G. Boffetta, A. Celani, and G. Falkovich, Nature Phys. **2**, 124 (2006).
[11] D. Bernard, P. Le Doussal, and A. A. Middleton (to be published).
[12] T. Jörg, J. Lukic, E. Marinari, and O. C. Martin, Phys. Rev. Lett. **96**, 237205 (2006).
[13] A. P. Young and A. K. Hartmann, Phys. Rev. B **64**, 180404 (2001).